A High-Power LED Driver Based on Single Inductor-Multiple Output DC–DC Converter With High Dimming Frequency and Wide Dimming Range

Yimeng Zhang, *Member, IEEE*, Guangjian Rong, Shasha Qu, Qingwen Song, *Member, IEEE*, Xiaoyan Tang, *Member, IEEE*, and Yuming Zhang, *Senior Member, IEEE*

***Abstract*—This article proposes an LED driver circuit which is wide-range continuous dimmable for high power lighting application. The proposed LED driver is based on single-inductor–multiple-output (SIMO) dc–dc converter. A pulsewidth modulation (PWM) control strategy is applied on the LED driver to control the brightness of LEDs flexibly and precisely, with which the dimming frequency can be increased significantly, and the dimming ratio for all branches can be adjusted separately. PWM dimming would cause the inductor current overshooting when dimming switch alters from OFF to ON, which makes the LED current varying. To suppress the inductor current overshooting, a sampling–holding circuit is adopted in the feedback loop of the proposed LED driver. A prototype of the proposed LED driver is fabricated and tested. The measurement results show that the dimming frequency can be increased to 10 kHz, the dimming ratio can be set from 5% to 100% with a minimum pulsewidth of 5 μs, and the inductor current overshooting is suppressed from 150% to approximately 0%. The proposed LED driver can output more than 80 W and achieve a conversion efficiency of 97%.**

***Index Terms*—High dimming frequency, inductor current overshooting suppression, LED driver, single-inductor–multiple-output (SISO), wide-range dimming.**

I. Introduction

LED has obvious advantages compared with the conventional illumination source, such as high luminous efficiency, energy saving, environmental protection, long lifetime, easy maintenance, and dimming ability, and its application prospect is very wide [1]–[3]. With the rapid development of LED lighting sources, the LED industry chain is also booming. Among them, LED driver power supply design is a key step in LED promotion and application because it affects the light efficiency, life, and cost of LED lamps. The LED is essentially a semiconductor diode with the same PN junction volt–ampere characteristics as a normal semiconductor diode, which means that the current of LED does not change with the forward voltage linearly. The temperature also affects the current. The higher the temperature is, the lower the barrier voltage becomes, which means the current becomes larger when the driving voltage is constant [4]. Therefore, the LED cannot be directly driven by the voltage source, the output current of the designed LED driver must be controlled precisely [5], [6].

For high-power LED display backlight applications, the output power of LED driver is required to be large enough. However, high output power will cause large size of system, and the brightness of LEDs is not easy to be controlled precisely. In order to control the current of the LEDs, and achieve compact and low-cost circuit, single-inductor–multiple-output (SIMO) dc–dc converter is adopted in LED driver [7]–[12]. The main circuit part has only one main inductor to provide output voltage for multiple outputs, which reduces the circuit size significantly. However, SIMO LED driver cannot be dimmable in a full range in dimming applications. To overcome the limitation of the LED dimming range, the pulsewidth modulation (PWM) is used to adjust the brightness of LED flexibly [13]–[16]. With the addition pulsewidth modulation (PWM) dimming switch, the dimming range can be extended to a larger range by using digital control strategy like using microcontrollers [17], but the algorithms are complicated and the cost increases. Furthermore, due to the limitation of microcontrollers, the dimming mode cannot be continuous, while the minimum ON time of the LEDs is still large, which limits the dimming frequency. The mainstream of dimming frequency for LEDs is about several hundred Hertz, which is not considered to be sensed by human eyes. However, the recent reports indicate that humans can feel LEDs flicking with low frequency PWM dimming mode in low duty cycle condition [18]. To solve this issue, increasing the dimming frequency is a feasible method. Moreover, for full range dimming with SIMO LED driver, there would be a time when the branch switch is OFF while the dimming switch is ON. During this time, the only power source is the output capacitors. To achieve a stable output current, large output capacitance is required for low dimming frequency application. However, in the high dimming frequency application, the time is shorter and the required output capacitance is smaller, which reduces the size of passive components.

Manuscript received June 27, 2019; revised September 18, 2019 and November 25, 2019; accepted January 26, 2020. Date of publication February 3, 2020; date of current version April 22, 2020. This work was supported by the National Science and Technology Major Project of China under Grant 2017-V-0014-0066. Recommended for publication by Associate Editor R. Hui. *(Corresponding author: Yimeng Zhang.)*

The authors are with the School of Microelectronics, Xidian University, Xi'an 710071, China (e-mail: zhangyimeng@xidian.edu.cn; 576968696@qq.com; 2570188749@qq.com; qwsong@xidian.edu.cn; xytang@mail.xidian.edu.cn; zhangym@xidian.edu.cn).

Color versions of one or more of the figures in this article are available online at https://ieeexplore.ieee.org.

Digital Object Identifier 10.1109/TPEL.2020.2971207

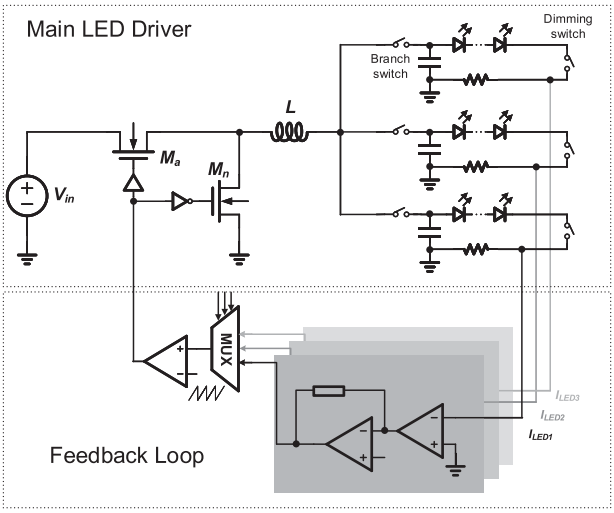

Fig. 1. PWM dimming LED driver based on Buck SIMO dc–dc converter.

PWM dimming strategy also brings inductor current overshooting which makes the brightness of LED vary due to unstable LED current [13]. In [13], an instant-duty-restoration (IDR) technique is proposed to solve this issue, but it is only applicable in low dimming frequency. Since at high dimming frequency, the IDR technique causes inductor current spike at dimming on instant when output current varies.

This article proposed a novel dimming switch control strategy based on SIMO dc–dc converter LED driver. With the proposed dimming strategy, the dimming range is extended to a wide range with fully analog control in theory with a dimming frequency of 10 kHz, and the inductor current overshooting is eliminated. A prototype is fabricated to demonstrate the proposal, and the measurement results show that a dimming range of 5% to 100% with minimum pulsewidth of 5 μs is achieved, and output power can reach 80 W with a peak efficiency of 97%. The inductor current overshooting issue is also solved with the proposed strategy.

II. Operation Principle of Proposed LED Driver

Fig. 1 illustrates a conventional LED driver with PWM dimming switch based on Buck SIMO dc–dc converter topology. For the SIMO LED driver, the time multiplexing technique [19]–[21] is adopted to avoid mutual interference between the multiple branches. Thus, the branches are sequentially turned ON, and the conduction times of any two branches cannot be overlapped. Therefore, the maximum duty ratio of the branch switch is 1/3 for three output branches condition. To output precise current, a feedback loop is necessary. A sampling resistor is used to convert LED current to sampling voltage in each branch. The sampling voltage is amplified to 10 times to achieve a voltage of V_e. V_e compares with a reference voltage in an error amplifier and the result is passed to the compensation network to achieve compensated voltage difference V_c. V_c is then compared with the sawtooth signal $V_{\rm saw}$ to generate PWM signal for Buck dc–dc control. With the feedback loop, the output current of LED driver can be controlled precisely. However, the mechanism

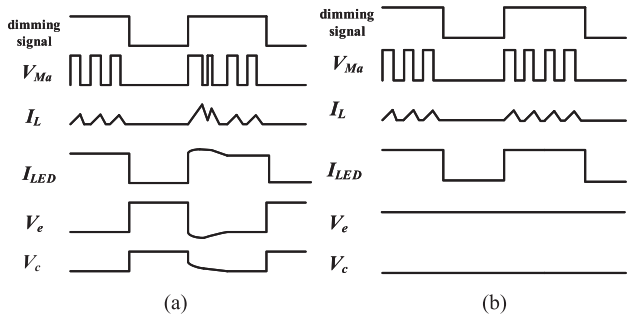

Fig. 2. Waveform diagram of (a) conventional and (b) proposed LED driver.

changes a little with adding dimming switch in the LED driver. The brightness of LEDs can be adjusted by turning ON/OFF of dimming switch. The LED current $I_{\rm LED}$ has a PWM waveform as same as the ON/OFF state of dimming switch, and its average current can be controlled by the duty ratio of the dimming signal as follows:

$$\overline{I}_{\rm LED} = I_{\rm LED} \times D_{\rm dim} \tag{1}$$

where $\overline{I}_{\rm LED}$ is the average LED current, and $D_{\rm dim}$ is the ON-duty ratio of the dimming switch.

A. Inductor Current Overshooting Suppression

During the dimming-OFFtime, if the dc–dc works normally, the output voltage of LED driver will keep increasing, which would make the LED current increase significantly in the next ON cycle. To avoid this issue, when the dimming switch is OFF, the main switch of dc–dc converter has to be turned OFF, too. As a result, the dc–dc converter doesnot work during the dimming-OFFtime, and the output voltage remains stable because of the output capacitor. This method is widely used to prevent LED driver's output voltage from increasing when output current is zero. However, the method is not flawless. Although the PWM signal is forced to 0 in dimming-OFFtime, the sampling circuits are still working. When the next ON time of dimming switch comes, the feedback loop works still based on a low sampled value, which causes the main switch to turn ON with a large ON-duty ratio. And the inductor current will increase dramatically, and the LED current will increase as a result. Fig. 2(a) illustrates the main signals' waveform diagram of the LED driver, and it shows how the inductor current overshooting during the ON/OFFtime of dimming switch.

In order to achieve a stable output current of LED, this article proposed a inductor current overshooting suppression technique based on SIMO LED driver with PWM dimming. As described above, with the conventional PWM dimming strategy, inductor current overshooting would occur which causes unstable brightness and affects the lifetime of LEDs. As analyzed above, the inductor current overshooting occurs because the feedback loop keeps working even during the dimming-OFF time. To stop the feedback loop sampling voltage during the dimming-OFFtime, a sample–hold (S&H) module and a multiplexer (MUX) are added in the feedback loop, as shown in Fig. 3. During the dimming-ON time, the S&H module samples voltage from the

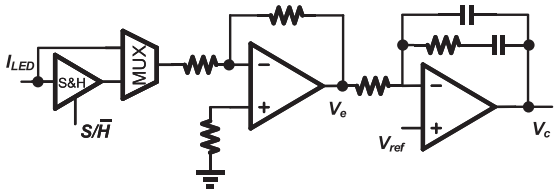

Fig. 3. Proposed feedback loop with S&H module.

sampling resistor, and the MUX outputs the sampled voltage directly to the error amplifier. Therefore, the feedback loop works in a same way as conventional LED driver, and the LED driver can provide a stable current during the dimming-ON time. During the dimming-OFFtime, the S&H module holds the last value of sampled voltage before the dimming switch turned OFF, and the MUX outputs this value to the error amplifier. At the beginning of the next dimming-ON time, the main switch will be controlled by the output PWM signal from the feedback loop based on the held value of the S&H module from the end of last dimming-ON time. With this strategy, the inductor current at the beginning of dimming-ON time will be almost the same as the value at the end of dimming-ON time in the last cycle. Fig. 2(b) illustrates the main waveform diagram of the description above.

B. Proposed LED Dimming Circuit Scheme and Control Principle

The proposed LED driver system can be divided into three units: Main power unit, feedback unit, and dimming control unit, which are illustrated in Fig. 4. For the SIMO circuit, in order to avoid cross interference between the branches, the discontinuous current mode (DCM) is usually used [22]–[24]. D_1, D_2, and D_3 are silicon carbide (SiC) diodes, which can avoid branch current backflow and reduce the ringing phenomenon generated in the DCM mode due to its low reverse recovery current [8]. Each LED string has 24 LEDs connected in series.

Fig. 5 illustrates the timing diagram of each switch in the system level. The timing relationship among switches requires the branch current not to interfere with each other, especially the currents from inductor to output capacitors and the output LED currents. The main switch M_a and the synchronous freewheeling switch M_n work at a same operating frequency with an opposite phase. Generally, the operating frequency of the main switch is much higher than that of branch switches, and the frequency of the branch switches is the same as the dimming switches. During the ON-time period of each branch, the main switch is in a continuous switching state, and the output voltage of the branch is controlled by the duty ratio of the main switch. When all the three branches are turned OFF, the main switch is turned OFF in the same instant, otherwise the inductor current may not be released and reversed. When any branch switch is turned ON, the corresponding dimming switch should also be turned ON, otherwise the voltage of the output capacitors C_1, C_2, or C_3 will increase. If the voltage across the capacitor exceeds the expected value, the output LED current $I_{\rm LED}$ will increase exponentially due to the *I–V* characteristics of LED, which will cause unstable brightness and shorter lifetime of LEDs. Therefore, for each branch, the branch switch must turn ON at the same instant when the dimming switch turns ON, and if the dimming ratio is less than 1/3, the branch switch must turn OFFwhen the dimming switch turns OFF. But when the dimming ratio is larger than 1/3, the dimming switch does not necessarily turn OFFwhen the branch switch turns OFF, because the output capacitor will provide the required current to LEDs. In addition, the duty ratio of the dimming switch on each branch can be adjusted separately. ON time of the three branches dimming switches can be overlapped and doesn't affect others. The relationship between the duty ratio of branch switch and dimming switch is defined as follows:

$$D_{M1,M2,M3} = \begin{cases} 1/3 & D_{M4,M5,M6} \geq 1/3 \\ D_{M4,M5,M6} & D_{M4,M5,M6} < 1/3. \end{cases} \tag{2}$$

The ON duty of the branch switch and the dimming switch is constrained as follows

$$0 \leq D_{M1,M2,M3} \leq 1/3 \tag{3}$$

$$0 \leq D_{M4,M5,M6} \leq 100\%. \tag{4}$$

C. Dimming Control Unit

Usually microcontrollers are used to achieve 0–100% wide dimming range and control timing relationship of switches. But microcontroller is a digital dimming method, which cannot output continuous dimming signal, and the dimming frequency and the minimum dimming pulsewidth is limited by its operation frequency. To achieve continuous dimming ratio, small dimming pulsewidth, and high dimming frequency, an analogue dimming control strategy is proposed to realize the control of the branch switches and the dimming switches. The schematic of dimming control unit is shown in Fig. 6. The counter determines the dimming frequency by both counted number and counter's operation frequency. The logic module is a combined digital circuit which generates control signals for branch switches and sawtooth wave generator based on the counted number. As shown in Fig. 6, D_1, D_2, and D_3 are signals for generating branch switches control signals, while W_1, W_2, and W_3 are control signals for sawtooth generators. As the time relationship of these signals, illustrated in Fig. 7, D_1, D_2, and D_3 have the same frequency and duty ratio of 1/3, with phase difference of $2\pi/3$ with each other, which makes sure that branch switches be not overlapped. W_1, W_2, and W_3 have exactly the same frequency and phase difference with D_1, D_2, and D_3, respectively, but their pulsewidth is short, i.e., one cycle of the counter's clock signal. As shown in Fig. 6, the sawtooth generator consists of a constant current source, a capacitor, and a switch. Taking W_1 as an example, when W_1 is low to turn OFF M_7, the current source $I_{\rm bias}$ will charge C_s linearly, so the voltage of $\rm SAW_1$ increases linearly from 0; when W_1 rises high to turn ON M_7, C_s will be discharged rapidly to 0 leading $\rm SAW_1$ dropping to 0. As a result, the voltage waveform of $\rm SAW_1$ is a sawtooth, whose frequency is the same as W_1. W_2 and W_3 work in the same way, and therefore, the rising point of sawtooth signals can be determined by W_1, W_2, and W_3. $\rm SAW_1$, $\rm SAW_2$, and $\rm SAW_3$ are compared with reference voltages $I_{\rm ref1}$,

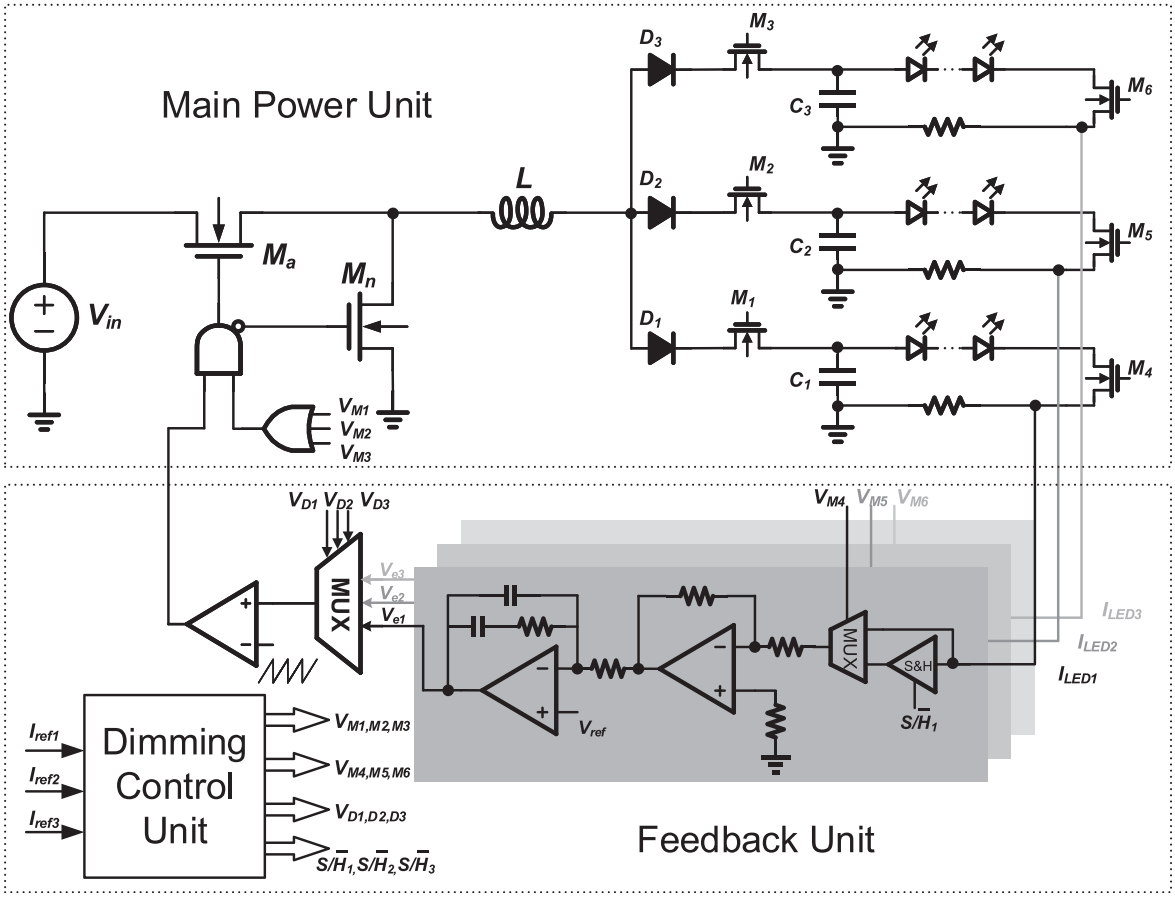

Fig. 4. Full schematic diagram of the proposed SIMO LED driver with the inductor current overshooting suppression technique.

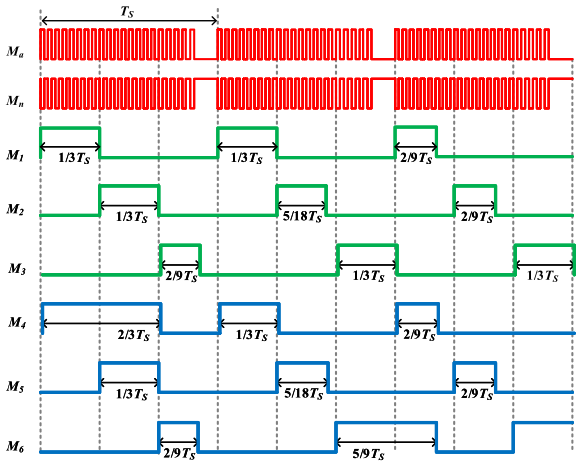

Fig. 5. Timing diagram of switches in the proposed LED driver.

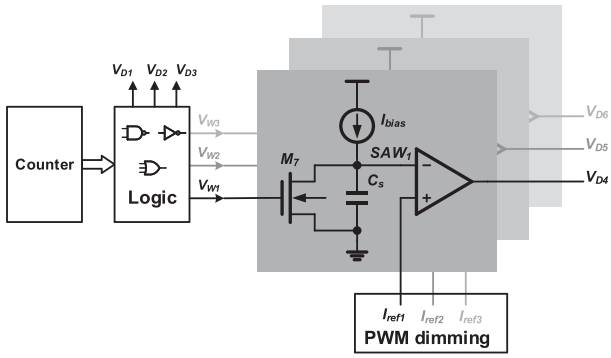

Fig. 6. Schematic of dimming control unit.

I_{ref2}, and I_{ref3} to generate D_4, D_5, and D_6 for dimming signals generation, respectively. By changing the reference voltages, duty cycle of dimming signals can be changed, as shown in Fig. 8.

As described above, a S&H module is used to stabilize the LED current during dimming-ON instant, which is also controlled by a logic signal. In order to sample and hold the LED current accurately, the module has to sample the value before the dimming signal falls down and hold it after the dimming signal rises up. Thus, there have to be a delay time t_d between sample–hold control signal ($S/\overline{H}$) and dimming signal in both rising edge and falling edge. Taking the first branch as an example, the circuit to generate the sample–hold signal $S/\overline{H}_1$, the control signal of branch switch M_1, and the control signal of dimming switch M_4 are shown in Fig. 9(a), and the timing relationship diagram is shown in Fig. 9(b). D_1 and D_4 rise up at the same instant of t_1. M_4 is achieved by delaying D_4 a time of

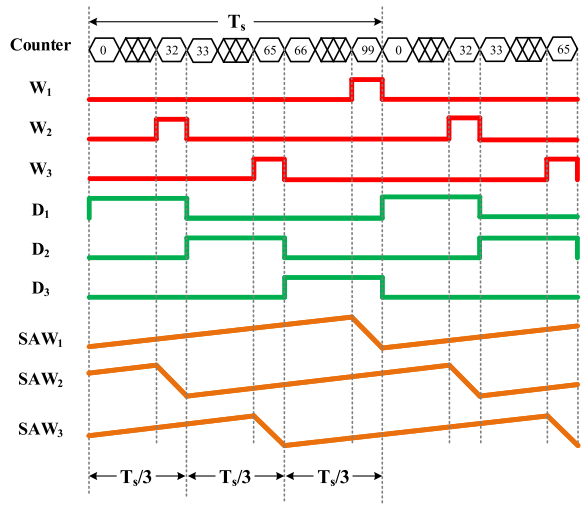

Fig. 7. Timing relationship of signals generated by the dimming control unit.

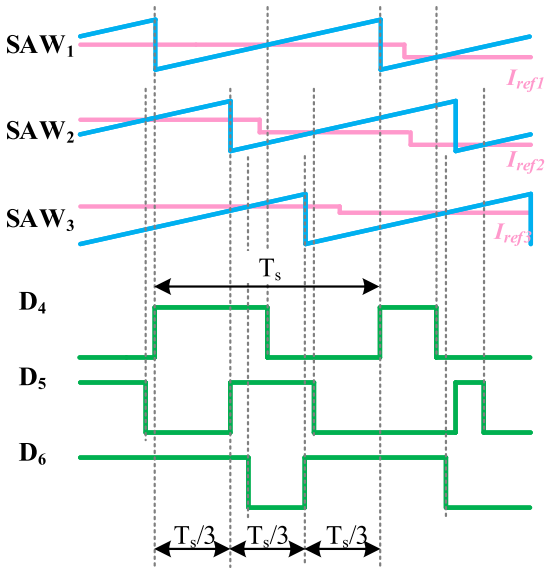

Fig. 8. PWM dimming signals generation.

$t_d = t_2 - t_1$. $S/\overline{H}_1$ is achieved by delaying M_4 another t_d, and ANDing the delayed signal with D_4. As a result, M_4 is one t_d ahead of $S/\overline{H}_1$ at the rising edge, and one t_d behind of $S/\overline{H}_1$ at the falling edge. D_1 is also delayed t_d to ensure the rising edge is synchronous with M_4, and the delayed signal is ANDed with M_4 to achieve M_1. It can be seen in Fig. 9(b) that when M_1 and M_4 have synchronous rising edge, and in the first cycle duty ratio of M_4 is larger than 1/3, then M_1 falls synchronously with D_1 delayed t_d, while in the second cycle duty ratio of M_4 is smaller than 1/3, then M_1 falls synchronously with M_4. This mechanism is according to the waveform shown in Fig. 7. It needs to be pointed out that the minimum pulsewidth of dimming control signal is limited the delay time t_d between M_4 and $S/\overline{H}_1$. The limitation due to the delay time is expressed as

$$D_{\min} = \frac{2t_d + t_{\rm sp}}{T_s} \tag{5}$$

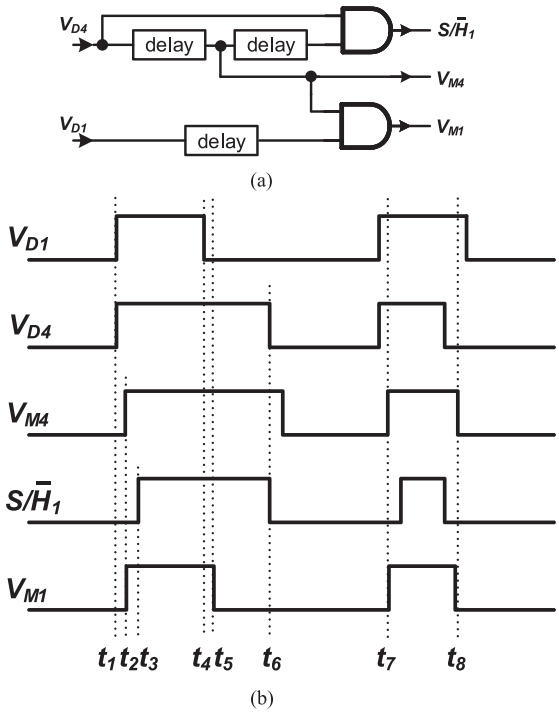

Fig. 9. Control signals of branch switch, dimming switch, and S&H module. (a) Schematic. (b) Waveform.

where T_s is the dimming period, and $t_{\rm sp}$ is the minimum sampling time for S&H module. In this design, t_d is set to 1.5 μs and $t_{\rm sp}$ is set to 2 μs to ensure the sampling–holding procedure of S&H module is sufficient. This value can be reduced by shrinking t_d and $t_{\rm sp}$, but the stability of S&H module cannot be guaranteed. Considering the wide dimming range and high dimming frequency, the dimming period is set to 20 times of minimum dimming-ON time, which results a dimming frequency of 10 kHz.

III. Analysis on Feedback Loop for High Frequency Dimming Application

Because low frequency PWM dimming method has the issue of LED flicker at low dimming ratio, high frequency PWM dimming control method is utilized in this work. However, as the dimming frequency increases, stability of the Buck SIMO dc–dc converter will be influenced. The stability of dc–dc converter is mainly controlled by the feedback loop. In order to achieve high frequency dimming LED driver, the characteristics of feedback loop is analyzed.

A. Design of Feedback Loop for Buck SIMO DC–DC LED Driver

The feedback loop consists of sampling resistors, amplifiers to amplify the sampled voltage, compensation networks for frequency compensation, and a comparator for main switch PWM signal generation, as shown in Fig. 4. The stability of dc–dc LED driver is mainly related to the compensation network. A typical design flow of compensation network is described in

TABLE I
CIRCUIT PARAMETERS OF PROPOSED LED DRIVER

Design Parameters	Value
Input Voltage	150 Vdc
Main Switch Frequency	200 kHz
Main Inductor	10 μH
Max Inductor Current Ripple	4 A
Output Capacitor	200 μF
Output Voltage	78 V
Rated LED Current	0.35 A
Dimming Frequency	10 kHz
Dimming Range	5%∼100%

the following. The parameters of the LED driver have to be determined, such as input voltage, output voltage/current, switching frequency, input/output capacitance, main inductor, load, etc. The parameters used in this article are listed in Table I. The main difference in the feedback loop comparing with conventional dc–dc is that a S&H module is added in the loop. However, this S&H loop doesn't affect the feedback analysis, because the feedback loop works normally in dimming-ON time, and stops in dimming-OFFtime, which works like that the feedback loop pauses during dimming-OFFtime, and resumes at dimming-ON instant. With this mechanism, the feedback analysis can be proceeded as normal. The transfer function of the Buck SIMO dc–dc LED driver is analyzed to calculate the zeros and poles. As mentioned above, the LED driver works in the DCM mode. The power stage transfer function of the Buck dc–dc in DCM mode is expressed as [25]

$$G_p(s) = \frac{i_o}{D} = \frac{\frac{2V_{oi}}{D} \times \frac{1-M}{2-M} \times \frac{1}{R_{\text{load}}}}{1 + \frac{2-M}{1-M} \cdot R_{\text{load}} C_o s} \tag{6}$$

where D is the duty ratio of main switch, R_{Load} is equivalent load resistance including equivalent resistance of LEDs and sampling resistor, C_o is output capacitance, and M is the DCM conversion ratio of Buck dc–dc given by

$$M = \frac{V_o}{V_{in}} = \frac{2}{1 + \sqrt{1 + \frac{8L}{R_{\text{load}} D^2 T}}} \tag{7}$$

where L is main inductance, and T is the period of main switch. The transfer function of PWM signal generator is $G_M(s)$ expressed as

$$G_M(s) = \frac{1}{V_{\text{osc}}} \tag{8}$$

where V_{osc} is the amplitude of sawtooth voltage. Usually the power stage and the PWM signal generator are combined for designability as plant, and therefore, the plant transfer function is $G(s)$ expressed as

$$G(s) = G_p(s) \times G_M(s) = \frac{\frac{2V_{oi}}{DV_{\text{osc}}} \times \frac{1-M}{2-M} \times \frac{1}{R_{\text{load}}}}{1 + \frac{2-M}{1-M} \cdot R_{\text{load}} C_o s}. \tag{9}$$

According to (9), the plant has no zero and one pole, which is related to M, R_{load}, and C_o, given by

$$f_p = \frac{1}{2\pi \cdot \frac{2-M}{1-M} \cdot R_{\text{load}} C_o}. \tag{10}$$

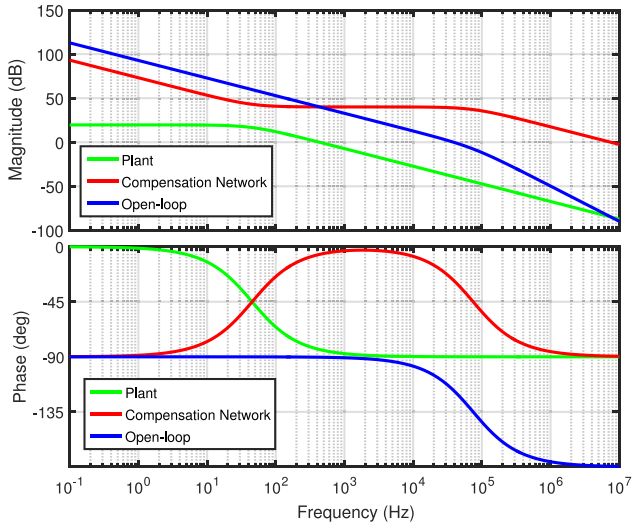

Fig. 10. Bode plots of the plant in Buck dc–dc LED driver.

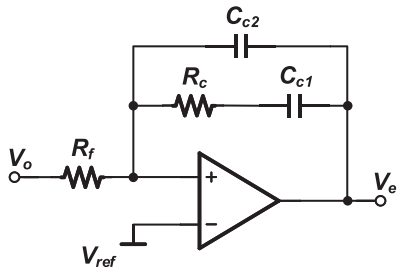

Fig. 11. Schematic of compensation network.

To illustrate the stability of the proposed system, a Bode plot is simulated with MATLAB. In general, Bode plot should be applied by considering extreme operation conditions, i.e., the light load and heavy load conditions. However, in the LED driver applications, the load is unchanged since the output current and voltage don't vary much when the number of LED lamps is determined. Therefore, the simulation is run with the output current of 0.35 A and the output voltage of 78 V.

The simulation of the plant transfer function is applied with parameters in this design, and the green curve in Fig. 10 shows its Bode plots. According to the Bode plots, it can be seen that the cross-over frequency is 443 Hz, which is far below the operation frequency of this design. In this design the operation frequency of main switch f is set to 200 kHz, while the dimming frequency f_d is 10 kHz. Usually, cross-over frequency f_0 of the LED driver is set to $0.1f$–$0.2f$, which is 20–40 kHz in this design. To make the system stable at the desirable f_0, a PI compensation network is utilized, as shown in Fig. 11. The transfer function of the compensation network is $G_c(s)$ expressed as

$$G_c(s) = \frac{V_e}{V_o}(s) = -\frac{1 + sR_cC_{c1}}{sR_f(C_{c1} + C_{c2})\left(sR_c\frac{C_{c1}C_{c2}}{C_{c1}+C_{c2}} + 1\right)}. \tag{11}$$

When selecting the parameters of these capacitors and resistors, C_{c1} is set to be much larger than C_{c2}, i.e., $C_{c1} \gg C_{c2}$.

As a result, $G_c(s)$ can be simplified to

$$G_c(s) \approx -\frac{1+sR_cC_{c1}}{sR_fC_{c1}(sR_cC_{c2}+1)}. \tag{12}$$

According to (12), the compensation network has one zero and two poles. The zero f_{z1} can be calculated as

$$f_{z1} = \frac{1}{2\pi R_cC_{c1}}. \tag{13}$$

One of the two poles is located at Origin, and the other one f_{p1} is calculated as

$$f_{p1} = \frac{1}{2\pi R_cC_{c2}}. \tag{14}$$

The zero f_{z1} is set to the position of f_p to increase the phase margin of the open-loop transfer function. The pole f_{p1} is set to be higher than f_0 to ensure enough phase margin. On the other hand, f_{p1} should be lower than main switching frequency f, so that the main switching ripple can be suppressed in output current. Usually f_{p1} is set to be $0.5f$. By selecting the parameters of R_f, R_c, C_{c1}, and C_{c2}, the zero and poles of compensation network can be adjusted to the designated position. The Bode plots of compensation network is the red curve shown in Fig. 10.

With the plant transfer function $G(s)$ and the compensation network transfer function $G_c(s)$, the open-loop transfer function $G_o(s)$ can be achieved as

$$G_o(s) = G_c(s) \times G(s). \tag{15}$$

The simulated Bode plots of the open-loop is the blue curve shown in Fig. 10. It can be observed that the phase margin is 62.6° at cross-over frequency of 38 kHz, which indicates that after the compensation the LED driver is stabilized at f_0.

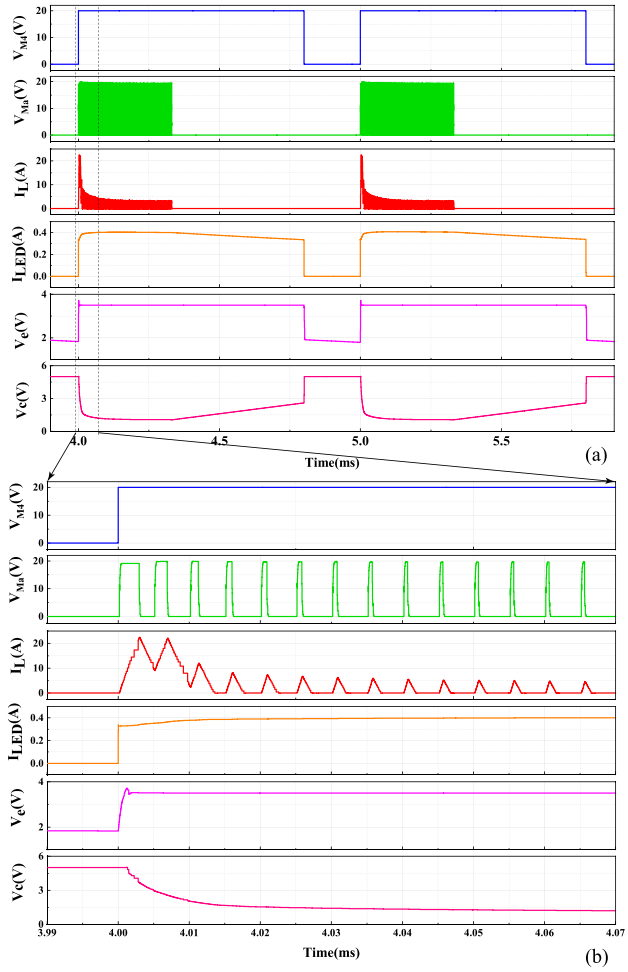

Fig. 12. Simulation waveforms of branch 1 with conventional PWM dimming control at a dimming frequency of 1 kHz. (a) Overview of two cycles. (b) Zoomed in view at dimming on instant.

B. Analysis on Stability of LED Driver With High Frequency Dimming

The open-loop in Section III-A is designed with a premise that the dimming ratio is 100%. After adding the dimming function, the stability of LED driver will change. From the OFF-state to the ON-state in every dimming cycle, it requires time for the output current of LED driver establishing from 0 to the designate value. In the state-changing time, sampled voltage from output changes, and the output of compensation network V_e changes from 0 to the reference voltage. As described in Section II-B, this would cause the output current to be unstable at the beginning of state changing. For low dimming frequency application, the current returns to the designated value before the dimming switch turns OFF. A simulation of conventional LED driver with dimming frequency of 1 kHz is applied for comparison. The dimming ratio is set to 80%, while the branch switching duty ratio is 1/3 according to timing relationship described in previous section. As shown in Fig. 12, at the beginning of the ON-state of dimming switch, the duty ratio of main switch increases to 25% while the value in stable state is 12%. This leads the peak value of inductor current I_L to a large value, and therefore, the LED current $I_{\rm LED}$ increases to 0.38 A with a large output capacitance of 200 μF. After several main switching period, the I_L falls back to a stable value, while the output $I_{\rm LED}$ falls gradually to the designate value of 0.35 A. Because the $I_{\rm LED}$ changes during a dimming-ON time, the LED driver is not applicable for high precision applications. Fig. 13 shows the simulation result with dimming frequency of 10 kHz, where the zero and pole of the compensation network are adjusted to an optimized position. The $I_{\rm LED}$ climbs to 0.41 A at the beginning of the ON-state of dimming switch, but the value never falls back to 0.35 A during a short dimming-ON time, which means for high dimming frequency application, the inductor current overshooting issue will be even more critical for high precision brightness application.

It can be seen that the $I_{\rm LED}$ peak value of 1 kHz dimming is larger than that of 10 kHz dimming. That's because the $I_{\rm LED}$ is supplied by output capacitance after the branch switch turns OFF. For 1 kHz dimming, the OFF-time interval of branch switch is longer, so the $I_{\rm LED}$ falls lower at the end of ON-time of dimming switch comparing with 10 kHz dimming. In the next ON-time cycle of dimming switch, the sampled voltage starts at a lower value, and the duty ratio of main switch is enlarged which causes a higher I_L. The inductor current overshooting issue not only

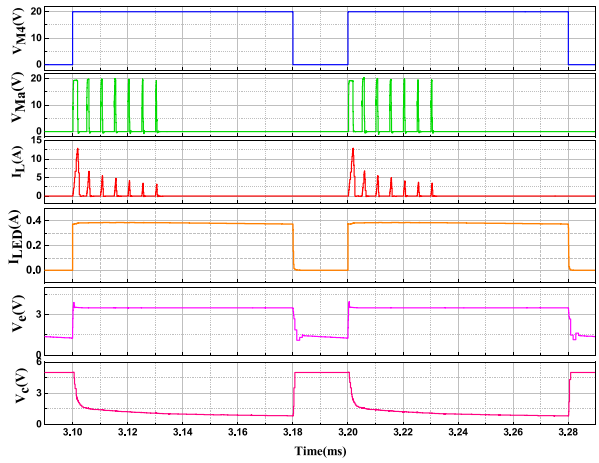

Fig. 13. Simulation waveforms of branch 1 with conventional PWM dimming control at a dimming frequency of 10 kHz.

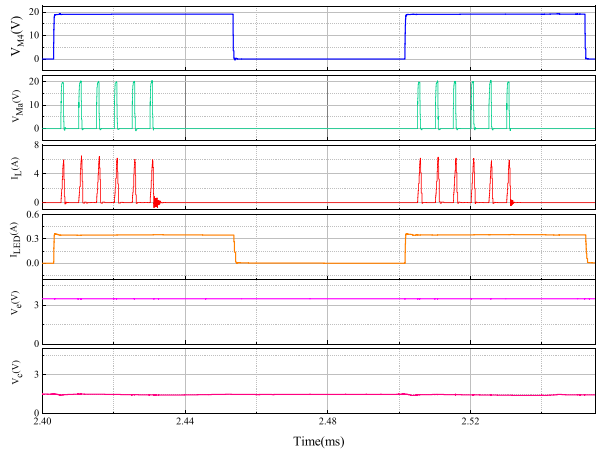

Fig. 14. Simulation waveforms of branch 1 with proposed dimming control at a dimming frequency of 10 kHz.

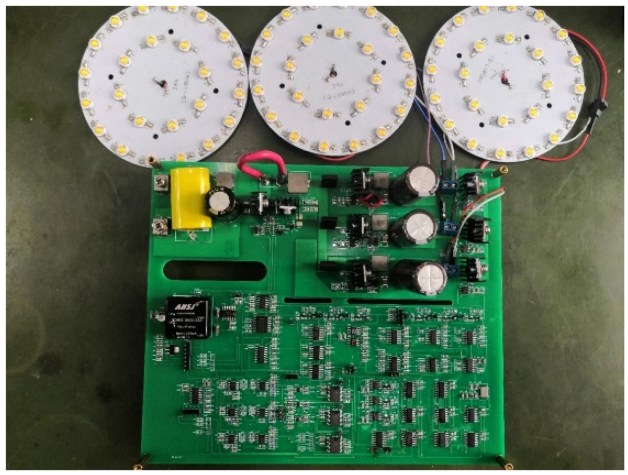

Fig. 15. Prototype of proposed SIMO LED driver.

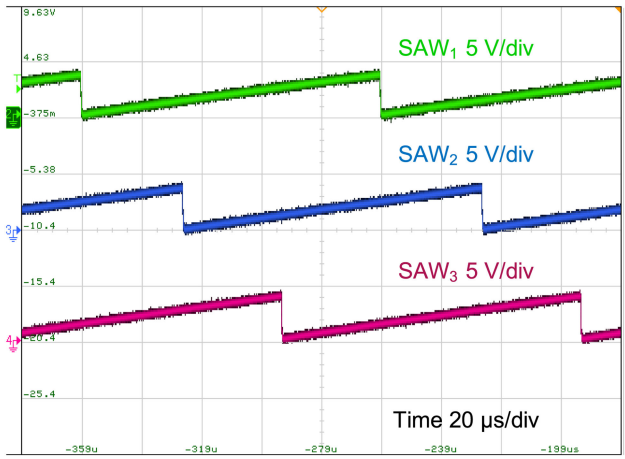

Fig. 16. Sawtooth wave to generate D_4, D_5, and D_6.

affects the $I_{\rm LED}$ at the beginning of ON time of dimming switch but also affects the $I_{\rm LED}$ during all the dimming ON-time. A simulation is applied on the proposed LED driver, and the result is shown in Fig. 14. The output of compensation network V_e is stored in a S&H module, and therefore the duty ratio of main switch at the beginning of dimming-ON is continuous with the end of last dimming-OFF time. The output current $I_{\rm LED}$ is stable at the designated value of 0.35 A.

IV. Performance Evaluation of Proposed LED Driver

To verify the proposed high frequency dimming strategy with inductor current overshooting suppression, an 80 W dc SIMO LED driver prototype with three branches was fabricated as shown in Fig. 15, and the schematic is shown in Fig. 4. As analyzed in previous sections, the circuit parameters are determined and shown in Table I. Comparing with [13], the main inductor is reduced from 5 to 4 μH, and output capacitors are reduced from 1000 to 200 μF, both of which are reduced significantly to achieve a same level current ripple due to high dimming frequency. Dimming ratio of each branch is adjusted by varying reference voltage $I_{\rm ref1}$, $I_{\rm ref2}$, and $I_{\rm ref3}$ in dimming control signal generator, shown in Fig. 6, which are given from external.

A. Dimming Control Unit Experimental Results

Fig. 16 shows the three sawtooth waves SAW$_1$, SAW$_2$, and SAW$_3$ generated by the dimming control unit. The frequency is 10 kHz and the amplitude is 3.3 V. The rising time point of each branch has 1/3 cycle difference with others. PWM signals D_4, D_5, and D_6 for dimming control are obtained by comparing the sawtooth waves SAW$_1$, SAW$_2$, and SAW$_3$ with the reference voltages $I_{\rm ref1}$, $I_{\rm ref2}$, and $I_{\rm ref3}$, respectively. D_4, D_5, and D_6 are shown in Fig. 17. As shown in Fig. 17, the rising time points of these signals also have 1/3 cycle time difference with others, which meets the requirement of synchronized conduction with branch switches. The ON time of three signals are different which demonstrates that the three branches can be dimmed separately, and the first branch shows the minimum pulsewidth of 5 μs which the proposed LED driver could achieve. Since the

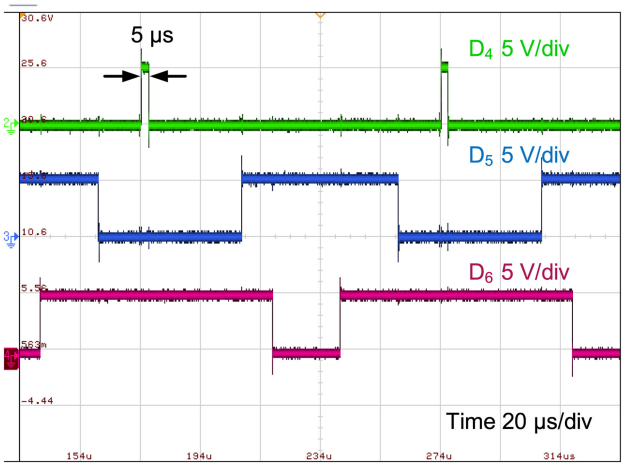

Fig. 17. Waveform of D_4, D_5, and D_6.

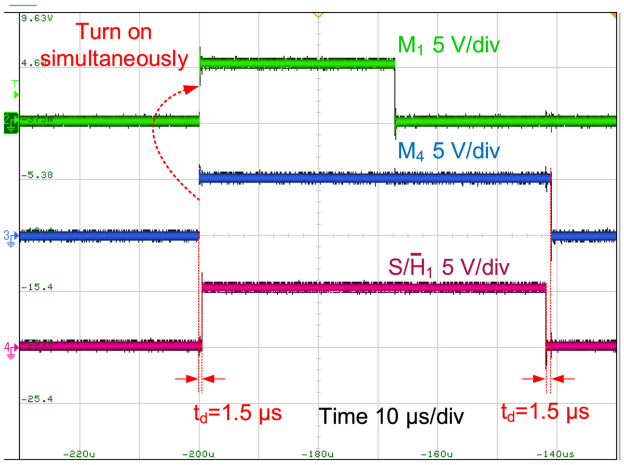

Fig. 18. Timing relationship of M_1, M_4, and $S/\overline{H}_1$.

dimming cycle is 100 μs, with the minimum 5 μs pulsewidth the minimum duty ratio is 5%.

Fig. 18 shows the tested timing relationship of branch switch control signal M_1, the dimming switch control signal M_4, and the sample–hold signal $S/\overline{H}_1$. M_1 and M_4 rises simultaneously, and there is delay time between M_4 and $S/\overline{H}_1$ at both rising edge and falling edge, which is corresponding with the description in Section II-C. The test results indicate that the timing control for branch switches, dimming switches, and sample–hold module are achieved as proposed.

B. Inductor Current Overshooting Suppression Experimental Results

In order to verify the proposed inductor current overshooting suppression strategy, the LED driver is tested both with conventional dimming strategy and the proposed strategy. The input of the driver is connected to a 150 Vdc voltage source. To compare the dynamic responses of the LED drivers, the output capacitance is reduced to 33 μF, and the measurement results are to verify if the output current returns to designate value in high

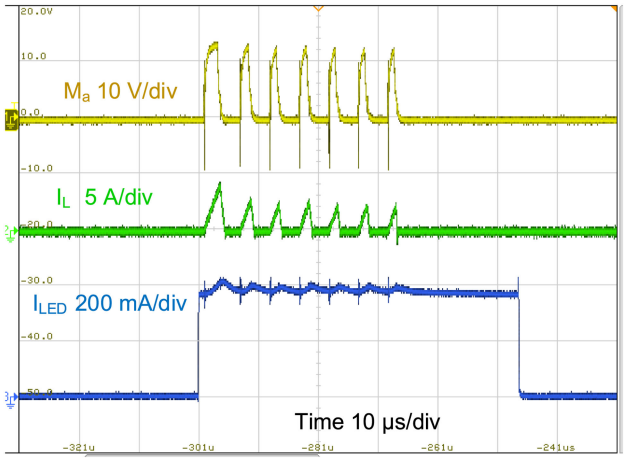

Fig. 19. Measurement results of $I_{\rm LED}$ with conventional dimming method.

dimming frequency condition with a smaller output capacitance. In this set of experiments, it was tested that only the first branch was turned ON, and the other two were deactivated by setting the dimming duty ratio to zero. The ON-state LED current is set to 0.35 A. Fig. 19 shows the test results of LED driver with the conventional PWM dimming technology. It can be seen that at the moment when the status of dimming switch is changing from OFFto ON, the first duty ratio of main switch gate signal is nearly 30%, while after several cycles it returns to a stable value of 12%. Therefore, the inductor current I_L spikes to 5 A with the 30% duty ratio, and then returns to 2 A when duty ratio returns to 12%. Because of the spike of I_L, $I_{\rm LED}$ rises to more than 0.4 A at the ON-instant, and then gradually falls with the output capacitance of 33 μF.

Due to the timing relationship of branch switch and dimming switch described previously, the duty ratio of branch switch is maximum 1/3. Because a high dimming frequency is adopted in the proposed LED driver, only seven cycles of main switch at most during the ON-time of branch switch. As a result, the spike on I_L affects the LED current significantly. The peak value of I_L is 2 A in stable status, and therefore, the current imbalance (IMC) can be expressed as follows

$$\text{IMC} = (I_{L\max} - I_{Ls})/I_{Ls} = 150\% \tag{16}$$

where $I_{L\max}$ is the maximum peak value of I_L, and I_{Ls} is the peak value of I_L when I_L goes stable.

Fig. 20 shows the experimental results of the LED driver after adopting the proposed strategy. The experiment was applied with a same condition with that applied in the measurement of Fig. 19. When the dimming switch is switched from the OFFstate to the ON state, the inductor overshoot current is effectively suppressed with the IMC value reducing to almost 0, and the LED current reaches the steady-state current with almost zero setting time. The inductor current ripple is stabilized at 2.5 A. By adopting the S&H module, output of the compensation network is stable at the beginning of dimming-ON time, so that the duty ratio of the main switch at this moment is the same as that at stable ON time, and the value is 12%.

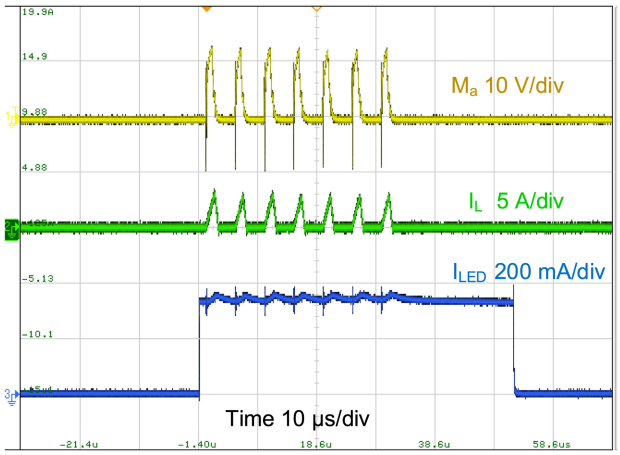

Fig. 20. Measurement results of I_{LED} with proposed dimming method.

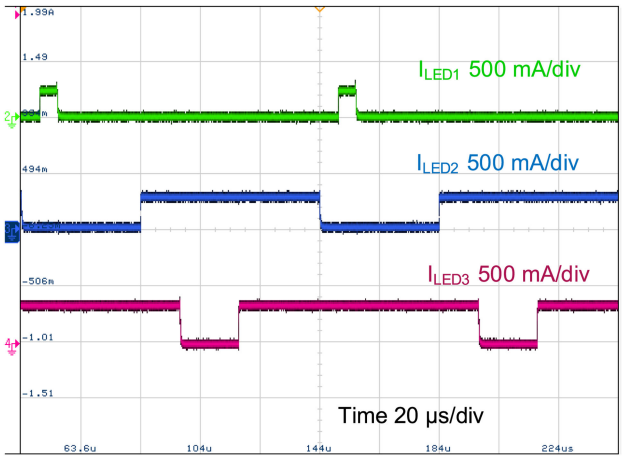

Fig. 21. Measured LED currents of the proposed LED driver.

C. Experimental Results of Complete Circuits

Fig. 21 is waveforms of measured current of three LED strings. The current of I_{LED1}, I_{LED2}, and I_{LED3} are stable at 0.35 A, and the duty ratio of the three LED strings current can be set separately. The dimming ratios for I_{LED1}, I_{LED2}, and I_{LED3} are set to 5%, 60%, and 80%, respectively, and ON time of I_{LED1} and I_{LED3}, I_{LED2} and I_{LED3} overlaps. It indicates that the dimming for each branch is independent and different continuous dimming ratio is achieved. The actual experiment can achieve a wide range of dimming of 5%–100% with a minimum dimming on pulsewidth of 5 μs. It can be noticed that both in Figs. 19 and 20 I_{LED} is a little fluctuant because of the small output capacitance of 33 μF. However, in the normal condition experiment, I_{LED} waveforms shown in Fig. 21 are smooth, since the output capacitance is changed to 200 μF.

Fig. 22 shows the measured power conversion efficiency of the proposed LED driver considering the power dissipation of analogue control circuits when the same dimming ratio is applied to all LED strings. The maximum output power for LED strings are at the level of 80 W. The measured efficiencies increase from 81% to 97%, and the peak value of 97.3% is achieved

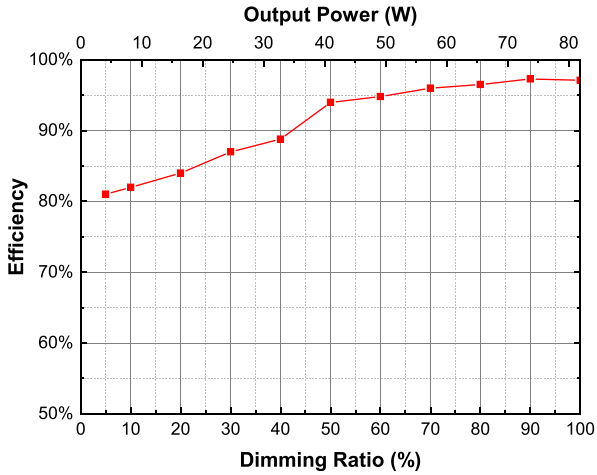

Fig. 22. Power conversion efficiency of proposed LED driver.

at 90% dimming ratio. At the low dimming ratio condition, the efficiency drops significantly, but it is still over 80%. This performance is better than continuous output SIMO dc–dc converter with same level output power, because at low dimming ratio condition, the main switch and synchronous switch are turned OFF during dimming-OFFtime, which decreases the power dissipation. The measurement result indicates that the proposed LED driver has a good performance on power conversion.

V. Conclusion

In this article, a wide-range dimmable high-power LED driver is proposed based on Buck SIMO dc–dc converter, which is compact and efficient. To overcome the low dimming ratio flicker issue with low frequency PWM dimming method, a high dimming frequency method is adopted in the proposed LED driver. The LED driver proposed in this article has three LED strings, each string can realize wide-range dimming of 5%–100% independently, with a dimming frequency of 10 kHz. In order to suppress the inductor current spike at dimming on instant, a S&H module is adopted to sample the output voltage during dimming ON-time and hold the sampled valued until the next dimming on instant. A prototype was fabricated to verify the improvement of the inductor current and the transient response performance. The measurement results show that it can achieve independent dimming of the three LED strings, and the peak power conversion efficiency of 97% is achieved.

References

[1] G. Z. Abdelmessih and J. M. Alonso, "A new active hybrid-series-parallel PWM dimming scheme for off-line integrated LED drivers with high efficiency and fast dynamics," in *Proc. IEEE Industry Appl. Soc. Annu. Meet.*, Oct. 2016, pp. 1–8.

[2] Y. Li and C. Chen, "A novel primary-side regulation scheme for single-stage high-power-factor ac-dc LED driving circuit," *IEEE Trans. Ind. Electron.*, vol. 60, no. 11, pp. 4978–4986, Nov. 2013.

[3] L. Wang, B. Zhang, and D. Qiu, "A novel valley-fill single-stage boost-forward converter with optimized performance in universal-line range for dimmable led lighting," *IEEE Trans. Ind. Electron.*, vol. 64, no. 4, pp. 2770–2778, Apr. 2017.

[4] Z. Dong, C. K. Tse, and S. Y. R. Hui, "Circuit theoretic considerations of led driving: Voltage-source versus current-source driving," *IEEE Trans. Power Electron.*, vol. 34, no. 5, pp. 4689–4702, May 2019.
[5] Y. Li *et al.*, "Fixed-frequency adaptive off-time controlled buck current regulator with excellent pulse-width modulation and analogue dimming for light-emitting diode driving applications," *IET Power Electron.*, vol. 8, no. 11, pp. 2229–2236, 2015.
[6] R. A. Pinto, J. M. Alonso, M. S. Perdigão, M. F. da Silva, and R. N. do Prado, "A new technique to equalize branch currents in multiarray LED lamps based on variable inductors," *IEEE Trans. Industry Appl.*, vol. 52, no. 1, pp. 521–530, Jan. 2016.
[7] X. Liu, Q. Yang, Q. Zhou, J. Xu, and G. Zhou, "Single-stage single-switch four-output resonant LED driver with high power factor and passive current balancing," *IEEE Trans. Power Electron.*, vol. 32, no. 6, pp. 4566–4576, Jun. 2017.
[8] J. Liu, H. Lv, Y. Zhang, Q. Song, Y. Zhang, and X. Tang, "Single-inductor multiple-output converter for high-power LED applications with independent current control based on SiC SBD," in *Proc. IEEE Appl. Power Electron. Conf. Expo.*, Mar. 2018, pp. 1192–1198.
[9] H. Wu, S. Wong, C. K. Tse, and Q. Chen, "A PFC single-coupled-inductor multiple-output LED driver without electrolytic capacitor," *IEEE Trans. Power Electron.*, vol. 34, no. 2, pp. 1709–1725, Feb. 2019.
[10] H. Chen, Y. Zhang, and D. Ma, "A SIMO parallel-string driver IC for dimmable LED backlighting with local bus voltage optimization and single time-shared regulation loop," *IEEE Trans. Power Electron.*, vol. 27, no. 1, pp. 452–462, Jan. 2012.
[11] A. T. L. Lee, J. K. O. Sin, and P. C. H. Chan, "Scalability of quasi-hysteretic FSM-based digitally controlled single-inductor dual-string buck LED driver to multiple strings," *IEEE Trans. Power Electron.*, vol. 29, no. 1, pp. 501–513, Jan. 2014.
[12] H. Kim, C. S. Yoon, H. Ju, D. Jeong, and J. Kim, "An ac-powered, flicker-free, multi-channel LED driver with current-balancing SIMO buck topology for large area lighting applications," in *Proc. IEEE Appl. Power Electron. Conf. Expo.*, Mar. 2014, pp. 3337–3341.
[13] S. Li, Y. Guo, S. Tan, and S. Y. Hui, "An off-line single-inductor multiple-output LED driver with high dimming precision and full dimming range," *IEEE Trans. Power Electron.*, vol. 32, no. 6, pp. 4716–4727, Jun. 2017.
[14] S. Li, Y. Guo, A. T. L. Lee, S.-C.-Tan, and S. Y. R. Hui, "Precise and full-range dimming control for an offline single-inductor-multiple-output led driver," in *Proc. IEEE Energy Convers. Congr. Expo.*, Sep. 2016, pp. 1–7.
[15] M. Doshi and R. Zane, "Control of solid-state lamps using a multiphase pulsewidth modulation technique," *IEEE Trans. Power Electron.*, vol. 25, no. 7, pp. 1894–1904, Jul. 2010.
[16] M. Tahan and T. Hu, "Multiple string LED driver with flexible and high-performance pwm dimming control," *IEEE Trans. Power Electron.*, vol. 32, no. 12, pp. 9293–9306, Dec. 2017.
[17] J. Huang, Q. Luo, Q. He, A. Zu, and L. Zhou, "Analysis and design of a digital-controlled single-stage series-type LED driver with independent n-channel output currents," *IEEE Trans. Power Electron.*, vol. 34, no. 9, pp. 9067–9081, Sep. 2019.
[18] H. Ahn, S. Hong, and O. Kwon, "A highly accurate current LED lamp driver with removal of low-frequency flicker using average current control method," *IEEE Trans. Power Electron.*, vol. 33, no. 10, pp. 8741–8753, Oct. 2018.
[19] K. Modepalli and L. Parsa, "A scalable n-color LED driver using single inductor multiple current output topology," *IEEE Trans. Power Electron.*, vol. 31, no. 5, pp. 3773–3783, May 2016.
[20] D. Ma, W. H. Ki, P. K. T. Mok, and C.-Y. Tsui, "Single-inductor multiple-output switching converters with bipolar outputs," in *Proc. ISCAS IEEE Int. Symp. Circuits Syst.*, vol. 2, May 2001, pp. 301–304.
[21] Y. Zhang and D. Ma, "A single-stage solar-powered LED display driver using power channel time multiplexing technique," *IEEE Trans. Power Electron.*, vol. 30, no. 7, pp. 3772–3780, Jul. 2015.
[22] R. K. Singh and R. Goel, "A novel lossless digital inductor current sensing technique based control implementation for switching dc/dc converter," in *Proc. IEEE Int. Conf. Ind. Technol.*, Mar. 2015, pp. 2030–2035.
[23] J. M. Alonso, M. A. D. Costa, and C. Ordiz, "Integrated buck-flyback converter as a high-power-factor off-line power supply," *IEEE Trans. Ind. Electron.*, vol. 55, no. 3, pp. 1090–1100, Mar. 2008.
[24] W. Yang, H. Yang, C. Huang, K. Chen, and Y. Lin, "A high-efficiency single-inductor multiple-output buck-type LED driver with average current correction technique," *IEEE Trans. Power Electron.*, vol. 33, no. 4, pp. 3375–3385, Apr. 2018.
[25] N. Mohan, T. M. Undeland, and W. P. Robbins, *Power Electronics*, 3rd ed. New Delhi, India: Wiley, 2003.

Yimeng Zhang (Member, IEEE) was born in China, in 1982. He received the B.E. degree in microelectronics from Tsinghua University, Beijing, China, in 2001, and the M.E. and Ph.D. degrees in system large-scale integrated (LSI) design from Waseda University, Fukuoka, Japan, in 2007 and 2012, respectively.

He is currently working as an Associate Professor with the School of Microelectronics, Xidian University, Xi'an, China. His current research interests include power electronics based on wide bandgap semiconductors.

Guangjian Rong was born in China, in 1995. He received the B.E. degree in microelectronics science and engineering from Changchun University of Science and Technology, Changchun, China, in 2017. Currently, he is working toward the M.S. degree with the School of Microeletronics, Xidian University, Xi'an, China.

Shasha Qu was born in China, in 1993. She received the B.E. degree in integrated circuit design and systems integration and the M.S. degree in integrated circuit engineering from Xidian University, Xi'an, China, in 2016 and 2019, respectively.

Qingwen Song (Member, IEEE) was born in China, in 1983. He received the B.S., M.S., and Ph.D. degrees in microelectronics engineering from Xidian University, Xi'an, China, in 2007, 2010, and 2012, respectively.

He is currently working as a Professor with the School of Microelectronics, Xidian University. His current research interests include SiC materials and devices.

Xiaoyan Tang (Member, IEEE) was born in China, in 1975. She received the M.S. and Ph.D. degrees in microelectronics engineering from Xidian University, Xi'an, China, in 2002 and 2008, respectively.

She is currently working as a Professor with the School of Microelectronics, Xidian University. Her current research interests include SiC materials and devices.

Yuming Zhang (Senior Member, IEEE) was born in China, in 1965. He received the B.S. degree in microelectronics from Tsinghua University, Beijing, China, in 1989, the M.S. degree in microelectronics from Xidian University, Xi'an, China, in 1992, and the Ph.D. degree in microelectronics from Xi'an Jiaotong University, Xi'an, China, in 1998.

He is currently working with the School of Microelectronics, Xidian University, as the Dean and a Professor. His current research interests include the materials, devices and circuit applications of silicon carbide semiconductors.